*Protein Science* (1995), *4*:1457–1469. Cambridge University Press. Printed in the USA.


# Characterization of a new four-chain coiled-coil: Influence of chain length on stability

ROBERT FAIRMAN, HANN-GUANG CHAO, LUCIANO MUELLER, THOMAS B. LAVOIE, LIYANG SHEN, JIRI NOVOTNY, AND GARY R. MATSUEDA

Division of Macromolecular Structure, Bristol-Myers Squibb Pharmaceutical Research Institute, Princeton, New Jersey, 08543-4000

(RECEIVED March 27, 1995; ACCEPTED May 31, 1995)

**Abstract**

Limited information is available on inherent stabilities of four-chain coiled-coils. We have developed a model system to study this folding motif using synthetic peptides derived from sequences contained in the tetramerization domain of Lac repressor. These peptides are tetrameric as judged by both gel filtration and sedimentation equilibrium and the tetramers are fully helical as determined by CD. The four-chain coiled-coils are well folded as judged by the cooperativity of thermal unfolding and by the extent of dispersion in aliphatic chemical shifts seen in NMR spectra. In addition, we measured the chain length dependence of this four-chain coiled-coil. To this end, we developed a general procedure for nonlinear curve fitting of denaturation data in oligomeric systems. The dissociation constants for bundles that contain $\alpha$-helical chains 21, 28, and 35 amino acids in length are $3.1 \times 10^{-12}$, $6.7 \times 10^{-23}$, and $1.0 \times 10^{-38}$ $M^3$, respectively. This corresponds to tetramer stabilities (in terms of the peptide monomer concentration) of 180 $\mu$M, 51 nM, and 280 fM, respectively. Finally, we discuss the rules governing coiled-coil formation in light of the work presented here.

**Keywords:** four-chain coiled-coil; four-helix bundle; monomer–tetramer equilibria

The coiled-coil protein structural motif has provided an important model for our understanding of the rules governing the folding and stability of proteins. In particular, much work has focused on the study of two-chain coiled-coils, with emphasis on the leucine zipper subclass, and less work has been directed toward the study of stability and folding of four-chain coiled-coils (Cohen & Parry, 1990). Four-chain coiled-coils might be considered as a subclass of the four-helix bundle motif. Four-helix bundles are a highly represented structural motif in proteins (cf. Harris et al., 1994) and, as such, this motif is one of the best understood protein folding motifs. The advantage of studying four-chain coiled-coils is that such a model system would provide a paradigm for understanding how the primary sequence dictates specificity of helix–helix interaction. Single-chain four-helix bundles are not readily amenable to this type of analysis because chain connectivity constrains helix–helix interactions.

Examples of well-studied four-chain coiled-coils include the bee venom protein, mellitin; a de novo designed protein, $\alpha$1 (Ho & DeGrado, 1987); and GCN4-pLI, a sequence variant of the leucine zipper domain from the transcription factor, GCN4 (Harbury et al., 1993). The stability and folding of mellitin, which forms antiparallel four-chain coiled-coils (Terwilliger & Eisenberg, 1982), has been studied extensively (Wilcox & Eisenberg, 1992; Hagihara et al., 1994); however, it will be difficult to generalize studies on mellitin because its structure deviates considerably from that of a canonical four-helix bundle. $\alpha$1B is also thought to form an antiparallel four-helix bundle and its folding has been studied in detail (Handel et al., 1993). Interestingly, both mellitin and $\alpha$1B have characteristics of molten globules, or compact intermediates, and thus, general principles about early steps in protein folding may be elucidated with these systems. A much more recent addition to the four-chain coiled-coil library is GCN4-pLI; this derivative of GCN4 forms all-parallel four-chain coiled-coils and extensive mutagenesis of the hydrophobic core of this structure is providing new insights into the rules governing oligomeric states of four-chain coiled-coils (Harbury et al., 1993).

We chose an amino acid sequence from the Lac repressor C-terminal oligomerization domain as a model system to study antiparallel four-chain coiled-coils. Lac repressor contains two distinct oligomerization domains, a dimerization domain and an immediately adjacent tetramerization domain, each containing a characteristic 4-3 hydrophobic repeat (Chakerian et al., 1991). These two domains are functionally separable; deletions

Reprint requests to: Robert Fairman, Division of Macromolecular Structure, Bristol-Myers Squibb Pharmaceutical Research Institute, P.O. Box 4000, Princeton, New Jersey 08543-4000; e-mail: fairman@bms.com.

in the last 32 amino acids of the Lac sequence result in Lac repressor protein that can form dimers but not tetramers (Chen & Matthews, 1992).

The positioning of the tetramerization domain at the C-terminus of Lac repressor suggests that it may be possible to isolate its function from the rest of the protein. Müller-Hill and his colleagues (Alberti et al., 1993) showed that recombinant peptides encoding the tetramerization domain of Lac repressor could form tetramers in the absence of the dimerization domain. Figure 1 illustrates the consequences of this 4-3 repeat on the formation of a four-helix bundle showing a helical wheel projection of the Lac repressor sequence from residues 339 to 359. There are seven residues per two turns of $\alpha$-helix in coiled-coils. By convention, individual heptads are designated **a**–**g**. In this nomenclature, the 4-3 hydrophobic repeat corresponds to positions **a** and **d**.

It is likely that antiparallel $\alpha$-helices make up the tetramer domain of Lac repressor. Lac repressor tetramers mediate the formation of DNA "looped complexes" (Brenowitz et al., 1991), thus the two dimers of Lac repressor most likely present their DNA-binding domains in an opposing fashion. An antiparallel arrangement of the putative helices at the tetramer interface accomplishes this. Further compelling evidence for antiparallel $\alpha$-helices comes from the work of Alberti and colleagues (1993) in their electrophoretic mobility shift studies of DNA sandwich complexes. However, in the strictest sense, this does not prove an antiparallel arrangement of the $\alpha$-helices in the absence of DNA because binding energy of the DNA–protein complex could, in principle, force such an antiparallel arrangement.

We synthesized peptides based on the Lac repressor C-terminal domain studied by Alberti and colleagues (1993) to determine their oligomerization states and to define their utility as models to study the forces governing four-chain coiled-coil stability.

## Results

We synthesized peptides corresponding to the sequence from the Lac repressor tetramerization domain (Table 1). The Lac 21 peptide contains residues 339–359 of Lac repressor with several modifications. The first three amino acids (MKQ) replace the wild-type sequence (PRA) and represent an artifact of the cloning strategy taken by Alberti and colleagues (1993) for their P2 protein. We retained these changes for three reasons: (1) to allow for N-terminal $\alpha$-helical extensions (proline is a helix-breaking residue); (2) to simplify the synthesis; and (3) to start with a sequence that has been demonstrated to form tetramers. Gly 359 likely acts as a helix stop signal in Lac repressor so we replaced this residue with alanine (a strong helix-forming amino acid) as the C-terminal residue. In addition, all peptides were acetylated at the amino-termini and amidated at the carboxy-termini in order to remove the unfavorable charge interactions with the helix dipoles (Shoemaker et al., 1987). Peptides Lac 28, Lac 29, and Lac 35 contain the Lac 21 sequence with either one or two additions of the central heptad of Lac 21 onto the amino-terminus. We synthesized these peptides to study the role of chain elongation on tetramer formation and stability.

First we wanted to know the oligomerization states of Lac 21, Lac 28, and Lac 35. The Lac 28 and Lac 35 peptides eluted from a Sephadex G50 gel-filtration column as symmetric, single peaks with molecular weights expected for tetramers (Fig. 2). In contrast, the shorter Lac 21 peptide eluted as an asymmetric peak

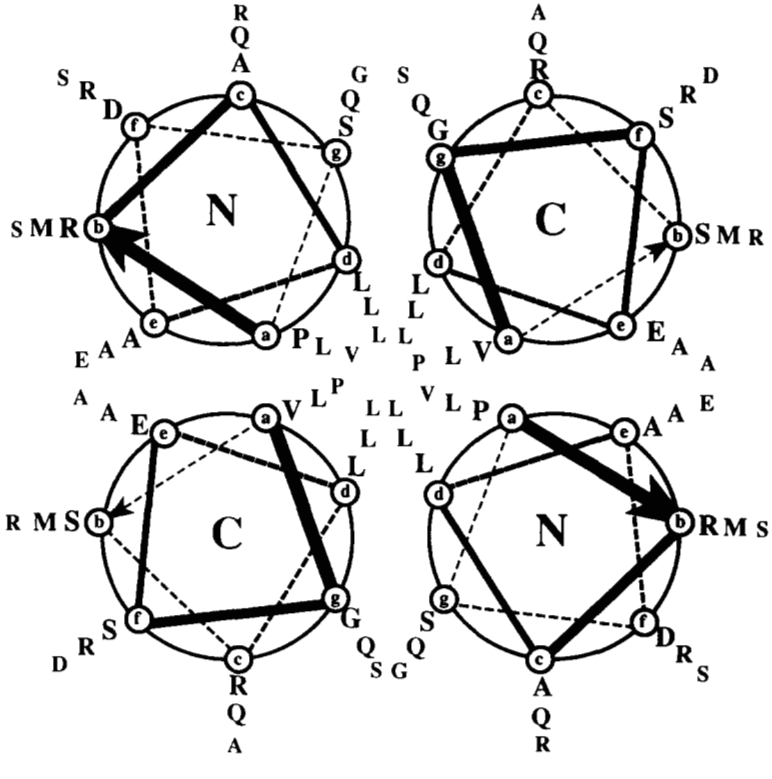


**Fig. 1.** Helix wheel diagram showing placement of C-terminal residues (339–359) of Lac repressor in a putative antiparallel four-helix bundle. Note that the helix is capped with a proline at the amino-terminus and a glycine at the carboxy-terminus; amino acids that are strong helix-breaking residues and often found at the ends of helices (Richardson & Richardson, 1988). Hydrophobic residues are revealed to be exclusively in **a** and **d** positions and are dominated by leucine, a residue commonly found in helical bundle proteins (Cohen & Parry, 1990).

**Table 1.** *Peptide sequences*

| Heptad position | | | a d | a d | a d |
|---|---|---|---|---|---|
| (wt Lac sequence: | | (339)- | PRALADS | LMQLARQ | VSRLESGQ) |
| Lac 24: | | Ac-YGG | MKQLADS | LMQLARQ | VSRLESA-$CONH_2$ |
| Lac 21: | | Ac- | MKQLADS | LMQLARQ | VSRLESA-$CONH_2$ |
| Lac 28: | Ac- | LMQLARQ | MKQLADS | LMQLARQ | VSRLESA-$CONH_2$ |
| Lac 29: | Ac-Y | LMQLARQ | MKQLADS | LMQLARQ | VSRLESA-$CONH_2$ |
| Lac 35: | Ac-LMQLARQ | LMQLARQ | MKQLADS | LMQLARQ | VSRLESA-$CONH_2$ |

with an apparent molecular weight of 5,000 Da, intermediate to the expected monomer (2,416 Da) and tetramer (9,664 Da) species (Fig. 2). This result for Lac 21 was somewhat surprising because the P2 protein from Alberti and colleagues (1993), which contains the Lac 21 sequence, was sufficiently stable to demonstrate tetramer formation by this technique. These results suggest that tetramers of Lac 28 and Lac 35, but not Lac 21, are stable in the micromolar concentration range.

We analyzed further the oligomerization states of Lac 21, Lac 28, and Lac 35 by sedimentation equilibrium (SE) ultracentrifugation as a second test of oligomerization because this technique does not suffer from shape dependence as does gel filtration. We subjected all three peptides to ultracentrifugation at three speeds and the data with their corresponding curve fits are shown in Figure 3B, C, and D. Both the Lac 28 and Lac 35 SE data are fitted using a single species analysis (Fig. 3C,D), where the molecular weight is included as a fitting parameter. The best-fit molecular weights for Lac 28 and Lac 35 are consistent with tetramer oligomerization states over the entire protein concentration gradient in the cell. The residuals from the Lac 28 curve fits are random at all three speeds. In contrast, there is a significant nonrandom component to the residuals from the curve fits to the 20,000-rpm and 30,000-rpm data for Lac 35. Addition of another term for a larger molecular weight species moderately improves the fit, although such a term predicts only trace amounts. To demonstrate the quality of the fit to a tetrameric species, we compare dimer, trimer, and tetramer single species analyses of the data for Lac 28 taken at 40,000 rpm (Fig. 3A). This speed would optimize the distribution of Lac 28 dimers and trimers and would provide the most sensitive probe of these oligomerization states. Significant nonrandom departures from the data are seen for the dimer and trimer fits, whereas the data are fit well to a tetramer species as judged either by direct observation of the curve fits or by the residuals generated from the curve fits.

SE analysis of Lac 21 confirmed the suggestion from gel filtration that this peptide is in dynamic equilibrium between monomer and tetramer states. Figure 3B shows Lac 21 data fitted with a monomer-tetramer equilibrium scheme. Global analysis of data taken at different temperatures revealed that the monomer-tetramer equilibrium is highly cooperative, with no improvement in fits by including a dimer term. A dissociation constant ($K_{41}$) could not be precisely determined because the goodness of fit for the data shown here is insensitive to $K_{41}$ within several orders of magnitude; however, the calculated $K_{41}$ is in the same range with the $K_{41}$ obtained from CD analysis (Fig. 5).

We next addressed the question of secondary structure in these peptides. The Lac 21 sequence is thought to encode for a coiled-coil structure in Lac repressor and this was tested by CD spectroscopy. Figure 4A and B show CD spectra for Lac 21. The two minima at 208 and 222 nm and the maximum at 192 nm demonstrate that Lac 21 is largely $\alpha$-helical (CD deconvolution of a Lac 21 spectrum is consistent with this conclusion). Spectra for Lac 28 and Lac 35 (not shown) also are predominantly $\alpha$-helical. Given the highly helical nature of these tetramers, it is very likely that these peptides form four-chain coiled-coils.

NMR spectra provide more information about the structures of the Lac peptides. We made two additional peptides for NMR studies (Lac 24 and Lac 29) containing the addition of a tyrosine at the amino-termini. Lac 24 contains a Tyr-Gly-Gly addition to the amino-terminus and was used, in conjunction with NMR analysis, for a careful comparison to Lac 21 to assure that tyrosine does not affect tetramer stability (CD data not shown).

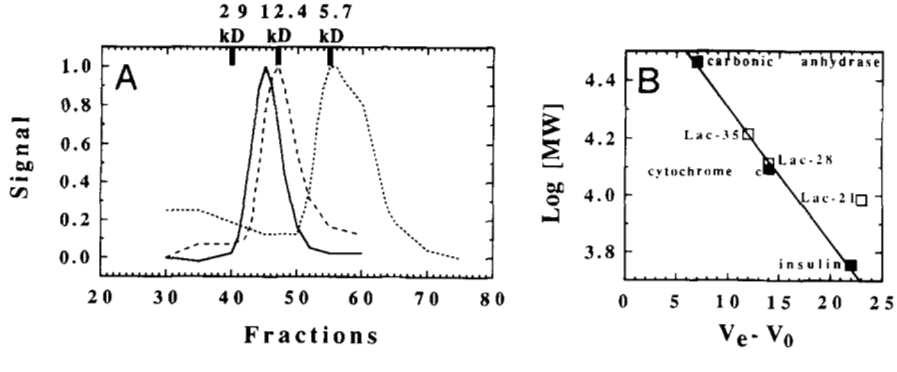


**Fig. 2.** Gel-filtration analysis of Lac 21, Lac 28, and Lac 35. **A:** Elution profiles are shown for each peptide and elution volumes for the standards are represented with bars at the top. **B:** The theoretical molecular weights of the Lac peptides are plotted against their elution volumes. The calculated molecular weights based on the curve generated by a linear least-squares fit to the standards shown are 16,300, 13,200, and 5,000 Da for Lac 35, Lac 28, and Lac 21, respectively. The expected tetramer molecular weights for these peptides are 16,400, 13,028, and 9,664 Da.

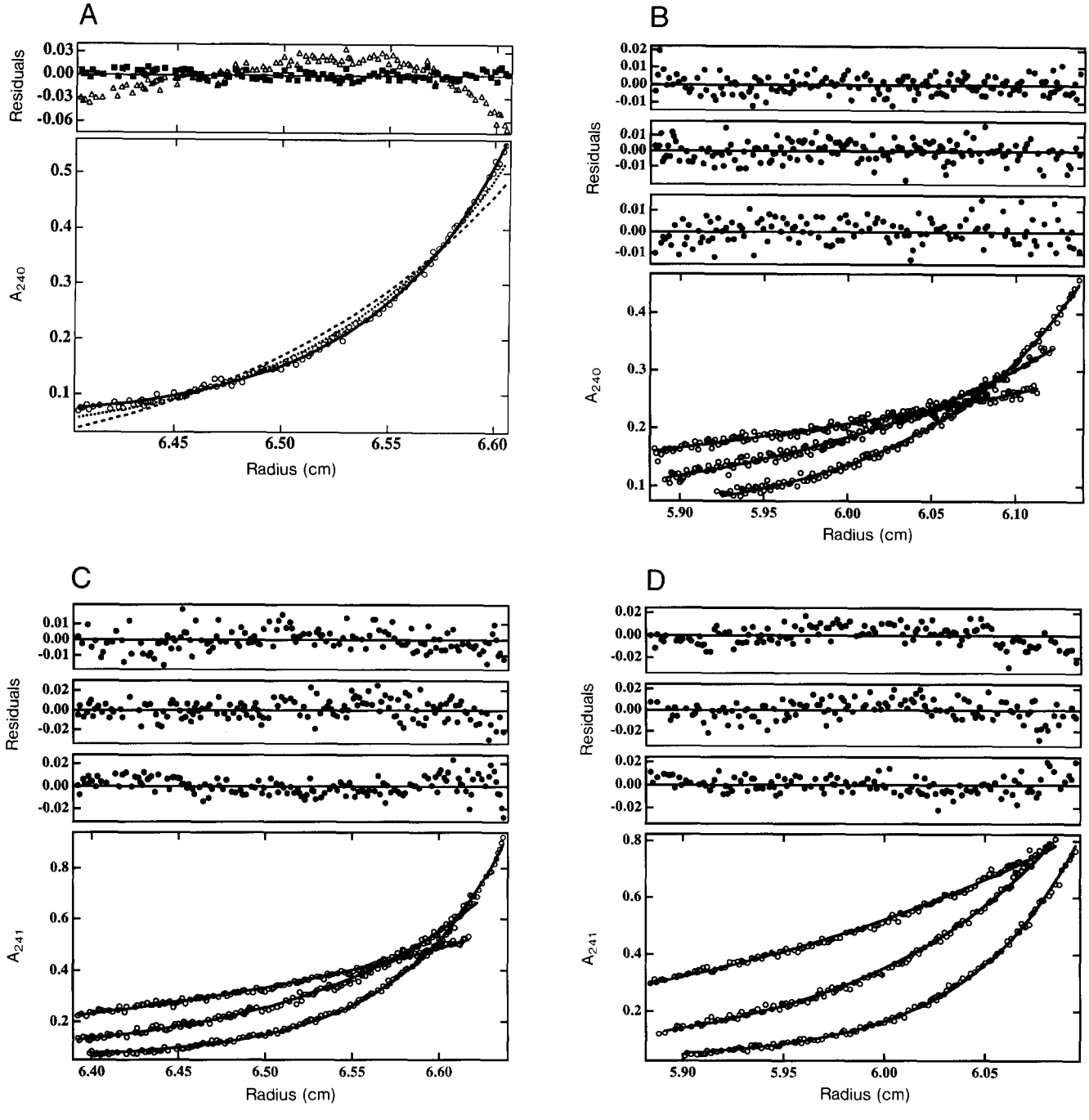


**Fig. 3.** Sedimentation equilibrium analysis of 200 $\mu$M each Lac 28 (A,C); Lac 21 (B); Lac 35 (D). Samples were run at 25 °C in 10 mM MOPS, pH 7.5, 100 mM NaCl. Rotor speeds used were 20,000, 30,000, and 40,000 rpm. **A:** Data for Lac 28 collected at 40,000 rpm are shown fitted with dimer (----), trimer (-------), and tetramer (——) species. Residuals from the curve fits are shown for the dimer and tetramer single species analysis. **B,C,D:** Curve fits for each peptide represent simultaneous fits for the three rotor speeds. Data for Lac 21 were fit to a monomer-tetramer equilibrium scheme, whereas data for Lac 28 and Lac 35 were fit using a single-species analysis and the aggregation states obtained from curve fitting are 4.2 and 3.9 for Lac 28 and Lac 35, respectively. Residuals from the curve fits are shown as well.

The insertion of glycines serves to avoid complications owing to interference of tyrosine CD absorption on measurements of $\alpha$-helix content when the amino-terminal residue of an $\alpha$-helix is tyrosine (Chakrabartty et al., 1993). Figure 6A shows the cross peaks between backbone amide hydrogen atoms and side-chain hydrogen atoms in a NOESY spectrum of Lac 24. The resolution of individual cross peaks is poor for this peptide. In order to rule out any role of the tyrosine in the quality of this spectrum, we collected a NOESY spectrum for Lac 21, and the resulting spectrum was virtually indistinguishable from that for

**Table 2.** *Curve-fitting parameters*

| Peptide | $K_{41}$ ($M^3$) | $\Delta G^{(H_2O)}$[a] | $m$[b] | $[\theta]_{mon}$[c] | $[\theta]_{tet}$[c] |
|---|---|---|---|---|---|
| Lac-21 | $3.1 \pm 0.7 (\times 10^{-12})$ | | | $-5.14 \pm 0.36$ | $-27.3 \pm 0.6$ |
| Lac-28 | $2.7 \pm 0.4 (\times 10^{-15})$ | | | $-2.45 \pm 0.28$ | $-27.9 \pm 0.3$ |
| Lac-28 | | $30.2 \pm 0.4$ | $-2.72 \pm 0.12$ | $-0.50 \pm 0.25$ | $-34.7 \pm 0.4$ |
| Lac-35 | | $51.8 \pm 1.1$ | $-3.94 \pm 0.16$ | $-4.02 \pm 0.36$[d] | $-31.7 \pm 0.1$ |

[a] Reported in kcal/mol.
[b] Reported in kcal/mol/M.
[c] $\times 10^{-3}$ (deg cm$^2$ dmol$^{-1}$).
[d] The lack of an experimental baseline for $[\theta]_{mon}$ results in an ill-defined curve-fitted value for this parameter. If a value of 0 is assumed for $[\theta]_{mon}$, then $\Delta G = 46.2$ kcal/mol.

Lac 24 (data not shown). Although the spectrum for Lac 24 has similar characteristics to that seen for many molten globule states of proteins, given the cooperative nature of its temperature unfolding profile (Lac 24 temperature unfolding was essentially identical to Lac 21 temperature unfolding; Fig. 4C), it is more likely that the poor resolution is a consequence of the low stability of Lac 24. Lac 24 has a tetramer stability that is significantly lower than 120 $\mu$M at pH 3.0 and we typically performed NMR experiments with 2 mM peptide. In this concentration range, Lac 24 peptide is most likely in fast exchange between unfolded monomer and folded tetramer.

There is a striking difference in the NOESY spectra of Lac 24 and Lac 29 (Tyr-Lac 28; Table 1). The spectrum of Lac 29 is representative of a protein with a well-defined tertiary fold (Fig. 6B). This result further supports the notion that the lower stability of Lac 24 is the main cause of its poorly resolved NMR spectrum. The quality of the NMR NOESY spectrum allows an evaluation of the helical nature of Lac 29. The NH-NH NOEs (Fig. 6C) are characteristic of well-defined $\alpha$-helices. Tentative assignment of NH-NH NOEs at the ends of the peptides suggests that the ends are $\alpha$-helical. In addition, the number of NH-$\alpha$H cross peaks is consistent with the number expected for a helix containing 29 residues and suggests that each helix is in an identical environment in the coiled-coil structure (containing either four- or twofold symmetry along the bundle axis). More detailed information about the structure of Lac 29 will require heteronuclear experiments because of the sequence degeneracy of the heptad repeats.

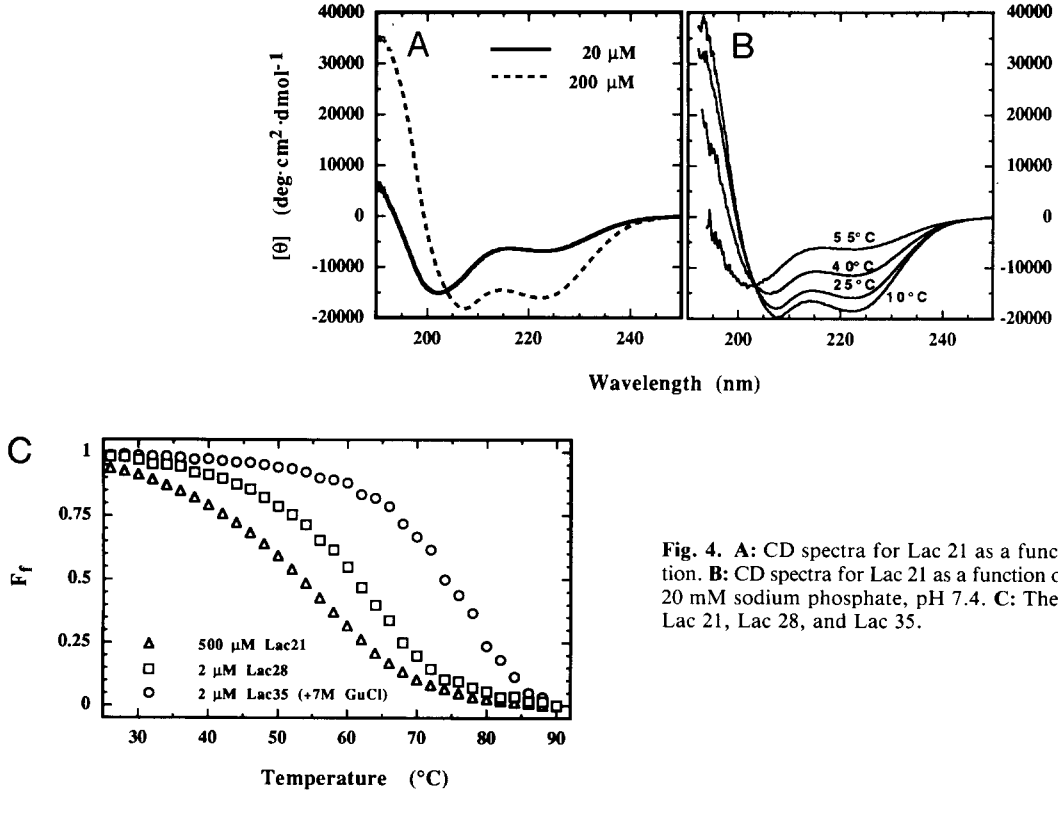


**Fig. 4. A:** CD spectra for Lac 21 as a function of peptide concentration. **B:** CD spectra for Lac 21 as a function of temperature. Conditions: 20 mM sodium phosphate, pH 7.4. **C:** Thermal unfolding curves for Lac 21, Lac 28, and Lac 35.

**Table 3.** *Tetramer stabilities*

| Peptide | $K_{41}$ ($M^3$) | $(M_T)_{1/2}$[a] (nM) | $\Delta G^{(H_2O)}$[b] | $\Delta G_m^{(H_2O)}$[b,c] |
|---|---|---|---|---|
| Lac 21 | $3.1 \times 10^{-12}$ | $1.8 \times 10^{+5}$ | 15.7 | 3.9 |
| Lac 28 | $6.7 \times 10^{-23}$ | $5.1 \times 10^{+1}$ | 30.2 | 7.6 |
| Lac 35 | $1.0 \times 10^{-38}$ | $2.8 \times 10^{-4}$ | 51.8 | 12.9 |
| | $(1.3 \times 10^{-34}$ | $6.3 \times 10^{-3}$ | 46.2 | 11.6)[d] |
| Lac 28[e]: | | | | |
| [Lac 28] | $2.7 \times 10^{-15}$ | $1.7 \times 10^{+4}$ | 19.9 | 5.0 |
| [GuCl] | $6.8 \times 10^{-16}$ | $1.1 \times 10^{+4}$ | 20.7 | 5.2 |

[a] $(M_T)_{1/2}$ is defined as the total monomer concentration for 50% tetramer dissociation (Bujalowski & Lohman, 1991).
[b] Reported in kcal/mol.
[c] $\Delta G$ is the $\Delta G$ per monomer.
[d] See note d in Table 2.
[e] The stability of Lac 28 in 3.5 M GuCl as measured either by the peptide concentration dependence method or by the GuCl denaturation method.

We hoped to gain further insight about the structure and symmetry of the Lac tetramers through a computer model-building exercise. We built the Lac 29 tetramer in three symmetries: all parallel (++++), parallel/antiparallel (++−−), and antiparallel (+−−+). The structure of the favored antiparallel model, showing the packing of the residues at the **a** and **d** positions, is shown in Figure 7A and Kinemage 1. We calculated and compared interhelical contact areas (total areas and those contributed by formally charged polar atoms) and electrostatic interhelical interactions for the three classes of models. Table 5 shows the results of these calculations. Overall, the total contact areas are comparable in all three cases but the all-parallel model shows a significantly larger contact surface contributed by the oxygen and nitrogen atoms of the formally charged side chains Arg, Lys, Asp, and Glu (by about 100Å$^2$, or approximately 30%). The buried charged side chains make close interactions (salt bridges) that are also responsible for the much higher apparent electrostatic stabilization of this model, −14.7 kcal compared to about −7.0 kcal for the other two models. However, buried salt bridges are extremely rare in native proteins, and so far have not been observed in α-helical oligomers. Thus, the buried salt bridges of the (++++) structure, although a natural outcome of side-chain modeling, driven in part, by optimization of Coulombic interactions, may be an indication that this tetrameric symmetry for the Lac sequence does not occur in nature.

The incorporation of tyrosine in both Lac 24 and Lac 29 also allowed us to test, using NMR, for near-space interactions between the N-terminal tyrosine and the C-terminal alanine. We observed NOEs between Tyr 1δε hydrogen atoms and Ala 29β hydrogen atoms of Lac 29. This set of NOEs suggests that the α-helices in Lac 29 are antiparallel with respect to one another. The shorter, Lac 24 peptide is also antiparallel based on similar NOEs between Tyr 1 and Ala 24 (data not shown). These data prompted us to evaluate the distances between Tyr 1 and Ala 29 in our models. After energy minimization of the Lac 29 structure, the shortest distances among the four pairs of Tyr 1 and Ala 29, in the antiparallel pairs of helices, ranged between 3.5 and 5.0 Å, consistent with the expected range from the NMR NOESY measurement for this amino acid pair (Table 6; Fig. 7B; Kinemage 1). Obviously, the Tyr 1–Ala 29 distance in parallel helical pairs is much larger.

Having established a basic structural understanding of the Lac peptides, we set out to measure rigorously the stability of these tetramers. We noted that the α-helix content in Lac 21 is dependent on peptide concentration (Fig. 4A), suggesting a linkage between α-helix formation and the monomer-tetramer equilibrium. Thermal analysis of CD spectra for Lac 21 further supports a strong linkage between these two processes. At elevated temperatures, the CD spectrum of Lac 21 takes on the appearance of a random coil, or unstructured peptide. An isodichroic point at 208 nm provides evidence that Lac 21 is in equilibrium between two states, an unstructured monomer and a structured tetramer. The thermodynamic analysis presented below assumes a two-state transition based on this evidence.

The stability of the tetramer is quantitated using the peptide concentration dependence of α-helix content as measured at 222 nm by CD (Fig. 5A) in an approach similar to that described by Ho and DeGrado (1987). These data were fit to various equilibrium schemes but the best fit is obtained using a simple monomer-tetramer equilibrium scheme according to Equation 1, and the curve fits in Figure 5A represent this scheme. The parameters determined from the curve fitting (the dissociation constant, $K_{41}$, and the CD signals for peptide monomer and tetramer, $[\theta]_{mon}$ and $[\theta]_{tet}$), along with their associated errors, are reported in Table 2. A more complex monomer-dimer-

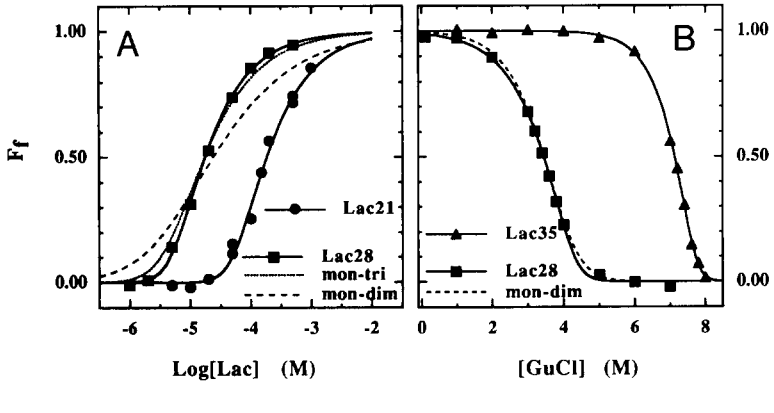


**Fig. 5.** Stabilities of Lac peptides. **A:** Peptide concentration dependences for Lac 21 and Lac 28 in 10 mM MOPS, pH 7.5, measured at 25 °C. It was necessary to add 3.5 M GuCl to Lac 28 samples in order to provide a CD window for measuring the binding isotherm. Data points represent an averaging time of 3 min. Lac 28 data are shown fit with monomer-tetramer (——), monomer-trimer (------), and monomer-dimer (----) equilibrium schemes for comparison. Lac 21 data are fit only to a monomer-tetramer equilibrium. **B:** GuCl denaturations of 10 μM Lac 28 and 2 μM Lac 35 in 10 mM MOPS, pH 7.5, measured at 25 °C. Given the stability of Lac 35, it was necessary to preincubate the samples at 37 °C for 5 days and at 25 °C for an additional 2 days prior to data acquisition to assure an equilibrium measurement. Data for Lac 28 are shown fit to monomer-tetramer (——) and monomer-dimer (----) equilibrium schemes. Lac 35 data are fit only to a monomer-tetramer equilibrium.

**Table 4.** *Comparison of stabilities with other four-helix bundles*

| Protein | Amino acids/helix | $\Delta G_{helix}^{(H_2O)}$ |
|---|---|---|
| Lac 21 | 21 | −3.9 |
| Lac 28 | 28 | −7.6 |
| Lac 35 | 35 | −12.9 |
| Mellitin[a] | 26 | −3.8 |
| ROP[b] | 27 | −4.3 |
| Peptide 2[c] | 16 | −4.5 |
| $\alpha_1$A[d] | 16 | −4.6 |
| $\alpha_1$B[d] | 16 | −5.5 |

[a] Wilcox and Eisenberg (1992)
[b] Steif et al. (1993)
[c] Chmielewski and Lipton (1994)
[d] Ho and DeGrado (1987)

**Table 5.** *Surface area changes and electrostatic energy change of the modeled Lac 29 in three symmetries: antiparallel (+−+−), parallel/antiparallel (++−−), and all-parallel (++++)*

| Tetramer (symmetry pattern) | $\Delta E_{el}$ (kcal/mol) | $\Delta S_{area}$ (Å$^2$) | $\Delta S_{area}^{p}$(R,K,E) (Å$^2$) |
|---|---|---|---|
| Lac 29 (±±) | −7.0 | 5,121 | 285 |
| Lac 29 (+±−) | −7.2 | 4,682 | 269 |
| Lac 29 (++++) | −14.7 | 4,945 | 379 |

tetramer scheme failed to improve the fits, further supporting the notion of a highly cooperative folding transition.

Lac 28 is too stable to monitor a peptide binding isotherm as described above for Lac 21. However, the tetramer of Lac 28 can be sufficiently destabilized by guanidinium chloride (GuCl), a potent chemical denaturant of proteins, to confirm the monomer-tetramer equilibrium behavior of this peptide. Figure 5A shows the peptide concentration dependence of α-helix content for Lac 28 in 3.5 M GuCl. The data are shown fit with monomer-dimer, monomer-trimer, and monomer-tetramer equilibrium schemes. For our model system, it is evident that CD analysis of oligomerization state is as sensitive a determinant as SE analysis (Fig. 3A).

We used an alternative approach to measure the stability of Lac 28 in $H_2O$: Figure 5B shows the GuCl concentration dependence of α-helix content for Lac 28. The numerical approach we have taken to curve fitting (see Materials and methods) allows for a simple extension of the equations to include a term describing the effects of GuCl on oligomeric systems (in principle, any perturbation of an oligomeric system that can be described by a mathematical function can be included, thus, this approach extends our abilities to study complex protein assembly processes). We fit the data in Figure 5B using Equation 4, which describes the denaturation of a monomer-tetramer system by GuCl. This curve fitting procedure takes advantage of the entire range of data and provides a more accurate estimate of $K_{41}$ than the standard approach using a linear transformation of the transition data with subsequent extrapolation of the [GuCl] dependence to 0 M. It is important to point out that good fits to GuCl denaturation data are insensitive to the oligomerization state (dimer and tetramer schemes fit equally well), so it is critical to determine independently the oligomerization states (i.e., gel filtration and/or SE). The stability of the Lac 28 tetramer in 3.5 M GuCl as measured by this method is in good agreement with the peptide binding isotherm approach (Table 3).

Lac 35 is significantly more stable than Lac 28. At 2 μM peptide, the lowest concentration readily detectable by CD, the mid-

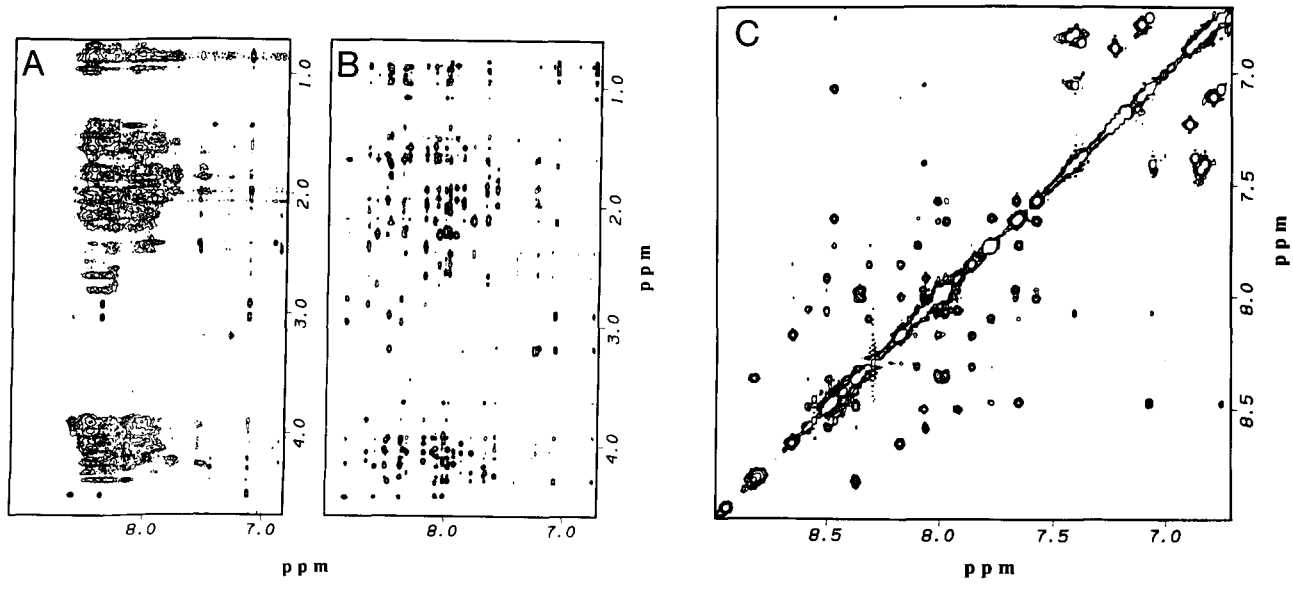


**Fig. 6.** NMR spectra. **A:** NH-CH region of Lac 24. **B:** NH-CH region of Lac 29. **C:** NH-NH region of Lac 29. Spectra were collected at 30 °C in 10 mM Na-phosphate, pH 3.0, 10% $D_2O$.

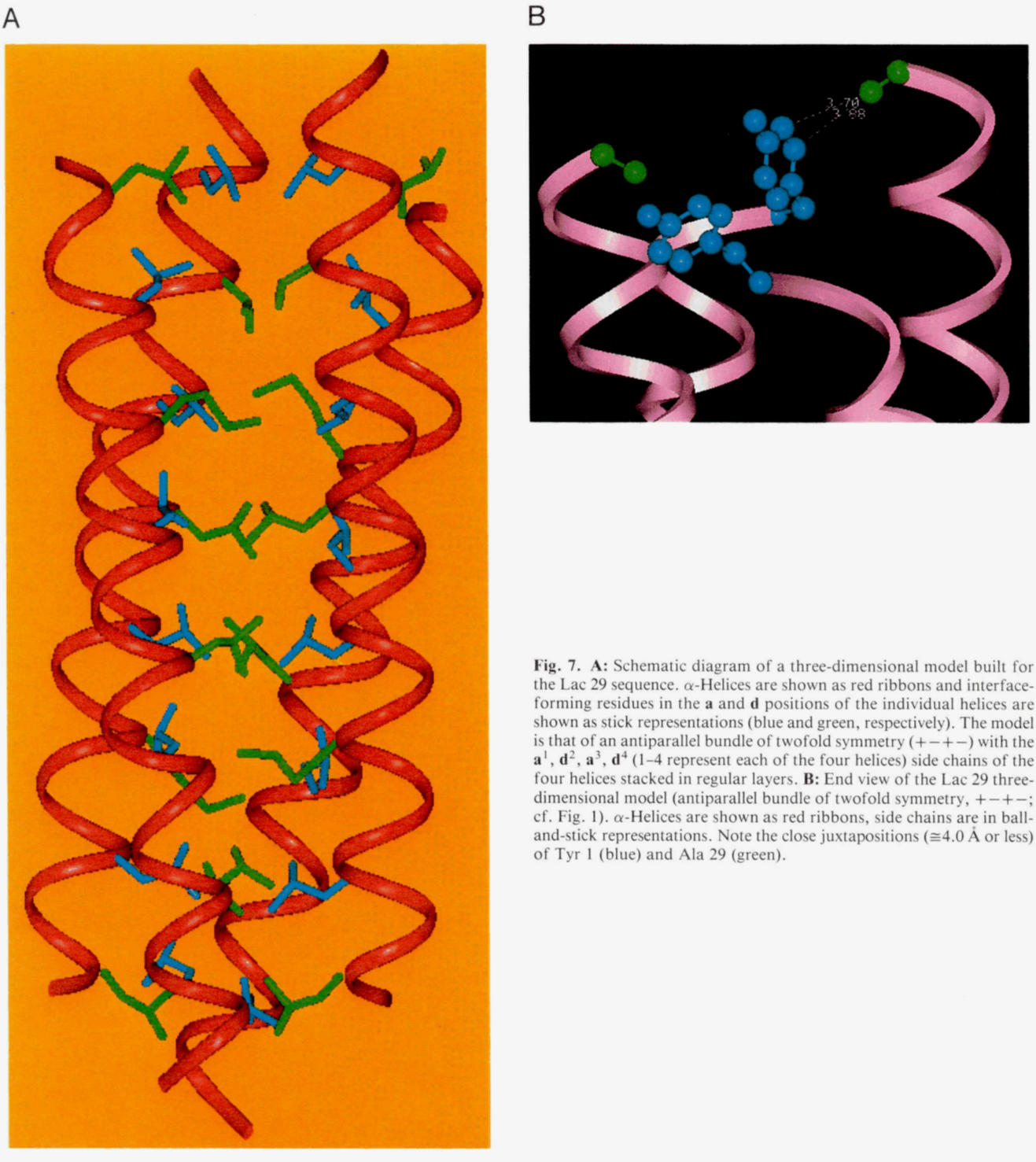


**Fig. 7.** **A:** Schematic diagram of a three-dimensional model built for the Lac 29 sequence. α-Helices are shown as red ribbons and interface-forming residues in the **a** and **d** positions of the individual helices are shown as stick representations (blue and green, respectively). The model is that of an antiparallel bundle of twofold symmetry (+−+−) with the $\mathbf{a}^1$, $\mathbf{d}^2$, $\mathbf{a}^3$, $\mathbf{d}^4$ (1–4 represent each of the four helices) side chains of the four helices stacked in regular layers. **B:** End view of the Lac 29 three-dimensional model (antiparallel bundle of twofold symmetry, +−+−; cf. Fig. 1). α-Helices are shown as red ribbons, side chains are in ball-and-stick representations. Note the close juxtapositions (≅4.0 Å or less) of Tyr 1 (blue) and Ala 29 (green).

point of the denaturation curve is about 7.5 M GuCl, therefore we cannot measure the monomer–tetramer cooperativity for Lac 35 by a peptide binding isotherm approach. The lack of a well-defined baseline for the unfolded monomer further exacerbates calculation of the stability of Lac 35. We report two values for $\Delta G$ in Table 3, that for the best-fit value of $[\theta]_{mon}$ and a value of 0 as a lower limit. Reversibility of Lac 35 unfolding is demonstrated by preparing samples from stocks of Lac 35 made in 0 M GuCl and 8 M GuCl. If the peptide stock in 8 M GuCl was irreversibly unfolded, then the apparent midpoint of the denaturation curve should fall below 4 M GuCl.

## Discussion

Using a multifaceted approach, we have identified and characterized a new four-chain coiled-coil structure based on the

**Table 6.** *Shortest distance of the four pairs of Tyr 1 and Ala 29 in modeled Lac 29 in three symmetries: Antiparallel (+−+−), parallel/antiparallel (++−−), and all-parallel (++++)*

| Tetramer (symmetry pattern) | Distance (Å) | | | | |
|---|---|---|---|---|---|
| | $C_\beta^A$-$C_\beta^Y$ | $C_\beta^A$-$C_{\delta 1}^Y$ | $C_\beta^A$-$C_{\epsilon 1}^Y$ | $C_\beta^A$-$C_{\delta 2}^Y$ | $C_\beta^A$-$C_{\epsilon 2}^Y$ |
| Lac 29 (±±) | 5.3 | 3.6 | 3.2 | 4.2 | 4.1 |
| Lac 29 (+±−) | 3.5 | 3.6 | 4.2 | 3.6 | 4.2 |
| Lac 29 (++++) | >38 | >38 | >38 | >38 | >38 |

C-terminal tetramerization domain of Lac repressor. Gel filtration, sedimentation equilibrium, and CD spectroscopy unequivocally demonstrate the tetrameric states of synthetic peptides derived from the native Lac repressor sequence. CD, in conjunction with NMR, shows that these tetramers are α-helical. NMR spectra also suggest a well-ordered tertiary structure for peptides Lac 29 and Lac 35. Although we do not yet have unambiguous evidence for the symmetry of these bundles, indirect evidence from Alberti and colleagues (1993) and from our NMR and modeling data strongly suggest that the helices of the bundle are antiparallel with respect to one another (see Kinemage 1).

Because we observe a strong linkage between the random coil–α-helix transition and the monomer–tetramer transition, we used CD to quantitate the stabilities of the four-chain coiled-coils. Evidence for an isodichroic point in the thermal analysis of Lac 21 (Fig. 4B) provided us with the impetus to apply a two-state thermodynamic treatment to peptide concentration isotherms and guanidine denaturation data. Although a more exact statistical mechanical description exists for the α-helix–random coil transition for monomeric α-helices and has been extended for two-chain coiled coils by Skolnick and Holtzer (1982), this approach has not been applied as yet to four-chain coiled-coils. However, several workers have suggested that, owing to the highly cooperative nature of the folding of coiled-coils, a two-state treatment is an accurate approximation of stability (O'Neil & DeGrado, 1990; Handel et al., 1993; Thompson et al., 1993). The sigmoidal shape of the thermal melting profile for Lac 21 further supports the cooperative nature of the folding transition. The thermal melting profiles of Lac 28 and Lac 35 suggest that these peptides fold highly cooperatively as well. The Lac peptides exhibit fully reversible temperature unfolding behavior, which is required for a thermodynamic analysis of these data. However, attempts to fit these data to the Gibbs–Helmholtz equation proved unsuccessful because $\Delta H$, $\Delta S$, and $\Delta C_p$ are highly interdependent.

The stability of Lac 21, the peptide most closely resembling the wild-type sequence, is −3.9 kcal/mol of monomer (Table 3). Although this stability is comparable to the stability of P2, a fusion protein containing the C-terminal portion of Lac repressor studied by Alberti and colleagues (1993), it is lower than the tetramer stability measured for intact Lac repressor (−5.3 kcal/mol/monomer, Royer et al. [1990]; −6.6 kcal/mol/monomer, Brenowitz et al. [1991]). This suggests that other protein–protein contacts in native Lac repressor are likely to be involved in stabilizing the tetramer further. Matthews and colleagues have argued that this C-terminal sequence forms a leucine zipper rather than a four-helix bundle in the context of native Lac repressor. Chen et al. (1994) show that lengthening the tetramerization domain of Lac repressor by inclusion of 1 or 2 heptads from the GCN4 coiled-coil sequence helps to stabilize dimerization of Lac repressor in the background of a Y282D mutant (which knocks out the dimerization domain). Because GCN4 forms a two-chain coiled-coil structure, it is not surprising that Lac repressor should favor dimerization. We would predict that our longer bundles would stabilize tetramer formation of Lac repressor, rather than dimer formation.

We have also measured the influence of chain length on the stability of the Lac four-chain coiled-coil. Analysis of Lac 28 and Lac 35 suggests that the addition of a heptad contributes approximately 4 kcal/mol per monomer of free energy (or 16 kcal/mol of tetramer). The consequence of this large free energy difference in the coiled-coils is that a wide range of stabilities can be accessed with small changes in sequence. This can be contrasted with the stabilities of dimeric coiled-coils, where the chain length dependence of stability is much smaller (Lau et al., 1984; Su et al., 1994). The wider range of stabilities for tetramers comes from the increased burial of hydrophobic surface relative to dimers. The stability of the Lac 21 tetramer is not unusual; other well-studied four-chain coiled-coils have comparable stabilities (Table 4). Inspection of Table 4 reveals no clear correlation between helix length and tetramer stability and probably reflects the importance of specific side-chain interactions on stability (cf. α1A and α1B; Ho & DeGrado, 1987). In contrast, Lac 28 and Lac 35 tetramers are much more stable; it will be possible to study subtle changes in stability because effects of mutations are magnified fourfold.

In order to understand how the Lac sequence encodes for a four-chain coiled-coil, it is useful to consider the rules that govern the assembly of coiled-coils. Clearly, the 4-3 hydrophobic repeat is not sufficient to distinguish oligomeric states or symmetry states of coiled-coils. Therefore, the specificity comes from the pattern of amino acids found at the interfacial **a**, **d**, **e**, and **g** positions of the coiled-coil heptad repeat.

The Lac sequence is dominated by leucine residues at the **a** and **d** positions; this is generally true for all coiled-coil sequences. Interestingly, the designed four-chain coiled-coil, α1B, contains leucines at the **a** and **d** positions, however, it has the characteristics of a molten globule, a state that is ill-defined in its tertiary structure (Handel et al., 1993). The molten globule state of α1B, while not fully understood, demonstrates that, although leucine residues at **a** and **d** positions may be critically important for stability, they are not the only determinant for defining specificity in the tertiary structure.

The **a** and **d** positions can also be important in defining the oligomeric states of coiled-coils. Harbury and colleagues (1993) showed that the placements of the hydrophobic residues, valine, leucine, and isoleucine, at **a** and **d** positions affect the oligomeric states of GCN4, an all-parallel coiled-coil. If we apply these rules

to the Lac 21 coiled-coil, on the assumption that the helices are all-parallel (three leucines at the **d** position; one leucine, one valine, and one methionine at the **a** position), it ought to form trimers with some dimer intermediate. However, we believe that the Lac peptides form antiparallel coiled-coils, therefore it is likely that the **a** and **d** positions must play a different role and different rules probably apply. Recall that in an all-parallel model, if one considers a plane orthogonal to the bundle axis, only **d**–**d** and **a**–**a** contacts are present, whereas in an antiparallel model, **a**–**d** contacts occur.

The **e** and **g** positions also are important in the assembly of four-chain coiled-coils (cf. Cohen & Parry, 1990; Alberti et al., 1993; Harbury et al., 1993; Krylov et al. 1994). These positions may play a dual role to influence the oligomer state as well as to potentiate the switch between parallel and antiparallel symmetries (Monera et al., 1994). It is thought that, when the **e** and **g** positions are dominated by alanine and/or small polar residues, as is seen in the Lac sequence, four-helix bundles will form and will be antiparallel. It has been suggested that, in this case, helix–dipole interactions would be the main driving force for the formation of antiparallel $\alpha$-helices (these dipole interactions could also play a role in maintaining the registry of helices in a bundle) (Sheridan et al., 1982; Robinson & Sligar, 1993). Krylov and colleagues (1994) find that mutation of **e** and **g** positions to alanine in the leucine zipper, VBP, causes a switch from dimers to tetramers and a similar experiment to convert **e** and **g** positions in GCN4 to alanines also results in a switch to tetramers (Alberti et al., 1993). Interestingly, when the **e** and **g** positions contain appropriately placed oppositely charged amino acids (cf. Cohen & Parry, 1990), four-helix bundles can be all-parallel (Harbury et al., 1993). The Lac sequence that we have used is dominated by alanine at position **e** and polar residues at position **g**. It would be informative to mutate residues in the **e** and **g** positions of the Lac tetramerization sequence to explore the importance of these positions for parallel versus antiparallel structures and dimer versus tetramer structures. Clearly, all four interfacial positions must be considered for understanding the fold of the Lac repressor coiled-coils because these positions seem to have a complex interplay in controlling oligomerization states. One must be cautious in overemphasizing any particular interfacial position.

Although specific positions in the heptad repeat are important for specificity of quaternary structure, the potential role of helix length in determining oligomeric states must not be overlooked. At first, we anticipated that a 21-residue $\alpha$-helix might simply be too short to form a stable dimeric coiled-coil (Lau et al., 1984; Su et al., 1994) and that extension to longer $\alpha$-helices may, at a minimum, stabilize a significantly populated dimer intermediate. Formation of tetramers in Lac 28 is highly cooperative, with no evidence for a dimer intermediate in its folding. Although we do not fully understand this surprising result, it provides further evidence that positional information of amino acid residues is a critical determinant for defining oligomerization states. The Lac four-chain coiled-coil model system will be useful for exploring these issues.

## Materials and methods

### *Peptide synthesis and purification*

Peptides were synthesized on an Applied Biosystem model 431A automated peptide synthesizer using the Boc/benzyl strategy. Peptidyl-resin was deprotected and cleaved by treatment with HF containing appropriate scavengers. Peptides were purified to homogeneity by reverse-phase HPLC (Chao et al., 1993) and their identity was established by amino acid analysis (Liu & Boykins, 1989) and electrospray or fast atom bombardment mass spectrometry analysis.

The concentrations of the peptides were determined by one or more of the following methods: (1) UV absorption in 6 M GuCl by the method of Brandts and Kaplan (1973); (2) quantitative amino acid analysis (Liu & Boykins, 1989); or (3) quantitative ninhydrin analysis (Rosen, 1957).

### *Gel filtration*

Peptides were loaded at 1 mM on a Sephadex G50 (coarse) resin column (1.6 × 95 cm) equilibrated in 10 mM 3-(*N*-morpholino)-propanesulfonic acid (MOPS) buffer, pH 7.5, 0.1 M NaCl, using a flow rate of 10 mL/h. The concentration of eluted peptides was typically 20-fold lower (40–50 $\mu$M). The column was calibrated with carbonic anhydrase (29,000 Da), cytochrome *c* (12,400 Da), human insulin (5,300 Da), and blue dextran 2000 (2,000,000 Da).

### *Ultracentrifugation*

Experiments were performed at 25 °C in a Beckman model XLA ultracentrifuge using an An 60 Ti rotor. Data for the Lac peptides were collected using six-channel Epon, charcoal-filled centerpieces with a 12-mm pathlength containing 110-$\mu$L samples and 125-$\mu$L buffer references. Peptide loading concentrations were 200 $\mu$M for Lac 21, Lac 28, and Lac 35 in 10 mM MOPS, pH 7.5, 0.1 M NaCl. Samples were centrifuged at 30,000, 40,000, and 50,000 rpm and protein distribution was monitored at a wavelength of 240 nm. Ten successive radial scans were averaged using a 0.001-cm step size and equilibrium was assumed if no change in distribution was observed at intervals of 2 h.

Data analysis software running under Igor (Wavemetrics, Lake Oswego, Oregon) and incorporating the algorithm of Michael L. Johnson (Johnson et al., 1981) was a generous gift from Preston Hensley (Smith Kline Beecham, King of Prussia, Pennsylvania). Partial specific volumes (Lac 21, 0.741; Lac 28, 0.745; Lac 35, 0.747) were calculated from the weight average of the partial specific volumes of the individual amino acids (Cohn & Edsall, 1946). Variation of the partial specific volume from 0.72 to 0.76 did not alter the predicted aggregation states of the peptides and proteins used in this study.

### *CD*

Data were collected using a Jasco-720 CD spectropolarimeter in the early phases of this work and an Aviv 62DS CD spectropolarimeter equipped with a thermoelectric device for temperature control for the majority of the studies. Spectra were collected on the Aviv instrument using a 0.25-nm step size, an averaging time of 2 s, and a bandwidth of 1.5 nm in 20 mM sodium phosphate, pH 7.4. All other measurements were made typically in 10 mM MOPS, pH 7.5, at 25 °C. Data points in the thermal melts represent a time average of 3 min. Samples for GuCl denaturation were prepared by mixing appropriate

amounts of two peptide stocks containing 0 M and 8 M GuCl (Pierce).

### *Data analysis*

Peptide concentration dependence data and GuCl denaturation data were fit by nonlinear least-squares methods with various equilibrium schemes using a PC version of the program MLAB (Civilised Software, Bethesda, Maryland) (Knott, 1979). The peptide concentration dependence data were fit according to the following relationship describing a tetramer → monomer equilibrium scheme (cf. Ho & DeGrado, 1987; Fairman et al., 1993):

$$[\theta]_{obs} = [\theta]_{mon} \times \frac{[monomer]}{[P_{tot}]} + [\theta]_{tet} \times \frac{4 \times [monomer]^4}{K_{41} \times [P_{tot}]}. \quad (1)$$

$[\theta]_{mon}$, and $[\theta]_{tet}$, and $K_{41}$ are the CD signal for the monomer, the CD signal for the tetramer, and the tetramer dissociation constant, respectively; these are treated as adjustable parameters by the curve-fitting routine. $[P_{tot}]$ is the concentration of peptide (independent variable) and $[\theta]_{obs}$ is the measured CD signal (dependent variable). Equation 1 ascribes the contributions of the peptide monomer and tetramer to the CD signal, $[\theta]_{obs}$, at a given concentration of peptide. The tetramer concentration is expressed in terms of the monomer in order to define Equation 1 in terms of a single unknown and to simplify the numerical analysis, according to the following relation:

$$[tetramer] = \frac{[monomer]^4}{K_{41}}. \quad (2)$$

The [monomer] term is determined for experimental $[P_{tot}]$ values and test values of $K_{41}$ by numerical solution of the mass balance equation:

$$[P_{tot}] = [monomer] + \frac{4 \times [monomer]^4}{K_{41}} \quad (3)$$

and the value for $K_{41}$ is then passed to the curve-fitting Equation 1 for fitting to the CD data.

A general procedure for nonlinear curve fitting of GuCl denaturation data for oligomeric systems is developed here. Previous curve fitting of such data has relied heavily on linearization by conversion of the measured signal to an equilibrium constant and then plotting the natural log of the equilibrium constant versus denaturant. Nonlinear approaches have been used for curve-fitting denaturation data of monomer–dimer systems because an analytical solution of the appropriate equilibrium expression is straightforward. However, for higher order equilibria, analytical solutions require formulas more complex than the simple quadratic formula. One way to avoid this problem is to take a combined numerical and nonlinear curve-fitting approach and the development of the appropriate expressions is described below.

The GuCl denaturation data are curve fit using the following modification of the monomer–tetramer Equation 1:

$$[\theta]_{obs} = [\theta]_{mon} \times \frac{[monomer]}{[P_{tot}]} + [\theta]_{tet} \times \frac{4 \times [monomer]^4}{e\left(\frac{\Delta G^{(H_2O)}}{-RT}\right) \times e\left(\frac{m[GuCl]}{-RT}\right)} \times \frac{1}{[P_{tot}]}. \quad (4)$$

The denominator of the second term is derived from the linear dependence of free energy, $\Delta G$, on GuCl concentration assuming a two-state solvent denaturation function (Santoro & Bolen, 1988):

$$\Delta G = \Delta G^{(H_2O)} + m[GuCl] \quad (5)$$

Equation 5 is introduced into the peptide monomer–tetramer equilibrium Equation 1 using the well-known relationship:

$$\Delta G = -RT \ln K_{41}. \quad (6)$$

### *NMR spectroscopy*

2D NOESY (Jeener et al., 1979; Kumar et al., 1980) were collected at 20 °C and 30 °C and mixing periods of 150 and 250 ms for the Lac 24 and Lac 29 peptides. Thirty-two scans were averaged per $t_1$-value and a total of 400 $t_1$-interferogram points were collected. The spectral widths were set to 7,000 Hz in both dimensions. All spectra were obtained on a Varian UnityPlus triple resonance spectrometer operating at 600 MHz proton frequency. The NMR sample consisted of 2–3 mM of peptide dissolved in 90% $H_2O$/10% $D_2O$, pH 3.0. Solvent peak suppression was accomplished by a 50-Hz CW presaturation during the relaxation delay of 1.5 s. Both $t_1$- and $t_2$-fids were apodized by a shifted squared sinebell function (90 °-shift and an 80 °-shift in $t_1$ and $t_2$, respectively) and zero-filled to 2,048 points prior to Fourier transformation. The spectra were processed with an in-house modified version of Felix 1.0 (Biosym Technologies).

### *Modeling*

Pilot computer experiments were conducted: (1) to build outline models of the Lac $\alpha$-helical tetramers; and (2) to estimate their relative stabilities. Antiparallel (+−+−), parallel/antiparallel (++−−), and all-parallel (++++) four-helix bundles of three and four Lac heptad repeats were built using the programs CONGEN (Bruccoleri & Karplus, 1987) and INSIGHT II (Biosym Technologies, Inc.). Helical backbones for the models were taken from GCN4-pLI, a parallel homotetramer formed by the mutated GCN4 leucine zipper sequence (Harbury et al., 1993). For the all-parallel (++++) Lac models, CONGEN was used to introduce the Lac side chains onto the GCN4 backbones by uniform conformational sampling of all the side-chain torsional degrees of freedom. The global minimum energy conformation for all the side chains was retained (the CONGEN side-chain search option ITER). To model the (+−+−) and the (++−−) oligomers, backbones of selected helices were rotated by about 180° around an axis perpendicular to the helical axis, to achieve an approximate antiparallel arrangement, and the skew angle

and the stagger (see below) of all the helix–helix pairs were systematically adjusted, prior to CONGEN side-chain construction by conformational sampling. Thus, families of stereochemically plausible models with different interhelical parameters were generated for all three tetrahelical symmetries considered.

Geometric parameters describing the structure and packing of four-helical bundles (Harris et al., 1994) are (1) helix polarity (parallel, antiparallel), (2) the helix–helix dihedral angles (usually comparable for all the helical pairs), (3) the skew angle, i.e., the relative angular orientation of two helices, and (4) the side-chain stagger, i.e., either in-register or staggered arrangement of identical heptad positions (layers) in the oligomer (e.g., the in-register, coplanar arrangement of the **a** and **d** position layers in all the helices, or a staggered alternation of the **a** position and **d** position layers; cf. Cregut et al., 1993). The known X-ray structures of bundles show a wide variety and combination of these parameters. So far, it has not been possible to choose a priori the parameters (points 1, 2, 3, 4 outlined above) of an unknown bundle structure, although, in many cases, plausible ranges of the helix dihedral angles and the skew angles can be identified based on the assumption of maximum interhelical contacts. In our Lac tetramer modeling, we limited ourselves to discrete sampling of helical arrangements with different skew angles and side-chain stagger. As a rule, we retained those models that optimized intrahelical side-chain packing in the hydrophobic positions **a** and **d**. As an approximate gauge of structural stability, the following values were calculated for each model: $i$, the total interhelical electrostatic Coulombic energy calculated with the effective dielectric constant, $\epsilon = 4r$, and $c$ the area of polar, formally charged atoms of the Arg, Lys, Asp, and Glu side chains that became buried at the interhelical interface.

## Note added in proof

The structure of Lac repressor core domain, including the tetramerization domain, has been reported (Friedman et al., 1995).

## Acknowledgments

We thank Paul Reiss for peptide purification, Clifford Klimas for amino acid analysis, Mark Hail for mass spectrometry analysis, and Jim Lear for encoding the MLAB algorithms. We also thank Jim Robertson for helpful discussions during the course of this work.

## References

Alberti S, Oehler S, von Wilcken-Bergmann B, Müller-Hill B. 1993. Genetic analysis of the leucine heptad repeats of Lac repressor: Evidence for a 4-helical bundle. *EMBO J 12*:3227–3236.

Brandts JF, Kaplan LJ. 1973. Derivative spectroscopy applied to tyrosyl chromophores. Studies on ribonuclease, lima bean inhibitors, insulin, and pancreatic trypsin inhibitor. *Biochemistry 12*:2011–2024.

Brenowitz M, Pickar A, Jamison E. 1991. Stability of a Lac repressor mediated "looped complex." *Biochemistry 30*:5986–5998.

Bruccoleri RE, Karplus M. 1987. Prediction of the folding of short polypeptide segments by uniform conformational sampling. *Biopolymers 26*:137–168.

Bujalowski W, Lohman TM. 1991. Monomer–tetramer equilibrium of the *Escherichia coli ssb-1* mutant single strand binding protein. *J Biol Chem 25*:1616–1626.

Chakerian AE, Tesmer VM, Manly SP, Brackett JK, Lynch MJ, Hoh JT, Matthews KS. 1991. Evidence for leucine zipper motif in lactose repressor protein. *J Biol Chem 266*:1371–1374.

Chakrabartty A, Kortemme T, Padmanabhan S, Baldwin RL. 1993. Aromatic side-chain contribution to far-ultraviolet circular dichroism of helical peptides and its effect on measurement of helix propensities. *Biochemistry 32*:5560–5565.

Chao HG, Bernatowicz MS, Matsueda GA. 1993. Preparation and use of the 4-[1-[*N*-(9-fluorenylmethyloxycarbonyl)-amino]-2-(trimethylsilyl)ethyl]phenoxyacetic acid linkage agent for solid-phase synthesis of C-terminal peptide amides: Improved yields of tryptophan-containing peptides. *J Org Chem 58*:2640–2644.

Chen J, Matthews KS. 1992. Deletion of lactose repressor carboxyl-terminal domain affects tetramer formation. *J Biol Chem 267*:13843–13850.

Chen J, Surendran R, Lee JC, Matthews KS. 1994. Construction of a dimeric repressor: Dissection of subunit interfaces in *Lac* repressor. *Biochemistry 33*:1234–1241.

Chmielewski J, Lipton M. 1994. The rational design of highly stable, amphiphilic helical peptides. *Int J Pept Protein Res 44*:152–157.

Cohen C, Parry DAD. 1990. α-Helical coiled coils and bundles: How to design an α-helical protein. *Proteins Struct Funct Genet 7*:1–15.

Cohn EJ, Edsall JT. 1946. *Proteins, amino acids and peptides as ions and dipolar ions*. New York: Reinhold Publishing Corp.

Cregut D, Liautard JP, Chiche L. 1993. Molecular modeling of coiled-coil α-tropomyosin: Analysis of staggered and in register helix–helix interactions. *Protein Eng 6*:51–58.

Fairman R, Beran-Steed RK, Anthony-Cahill SJ, Lear JD, Stafford WF, DeGrado WF, Benfield PA, Brenner SL. 1993. Multiple oligomeric states regulate the DNA binding of helix-loop-helix peptides. *Proc Natl Acad Sci USA 90*:10429–10433.

Friedman et al. 1995. *Science 264*:1721–1727.

Hagihara Y, Oobatake M, Goto Y. 1994. Thermal unfolding of tetrameric mellitin: Comparison with the molten globule state of cytochrome *c*. *Protein Sci 3*:1418–1429.

Handel TM, Williams SA, DeGrado WF. 1993. Metal ion-dependent modulation of the dynamics of a designed protein. *Science 261*:879–885.

Harbury PB, Zhang T, Kim PS, Alber T. 1993. A switch between two-, three-, and four-stranded coiled coils in GCN4 leucine zipper mutants. *Science 262*:1401–1407.

Harris NL, Presnell SR, Cohen FE. 1994. Four helix bundle diversity in globular proteins. *J Mol Biol 236*:1356–1368.

Ho SP, DeGrado WF. 1987. Design of a 4-helix bundle protein: Synthesis of peptides which self-associate into a helical protein. *J Am Chem Soc 109*:6751–6758.

Jeener J, Meier BH, Bachmann P, Ernst RR. 1979. Investigation of exchange processes by two-dimensional NMR spectroscopy. *J Chem Phys 71*: 4546–4553.

Johnson ML, Correia JJ, Yphantis DA, Halverson HR. 1981. Analysis of data from the analytical ultracentrifuge by nonlinear least-squares techniques. *Biophys J 36*:575–588.

Knott GD. 1979. MLAB—A mathematical modeling tool. *Comput Programs Biomed 10*:271–280.

Krylov D, Mikhailenko I, Vinson CR. 1994. A thermodynamic scale for leucine zipper stability and dimerization specificity: e and g interhelical interactions. *EMBO J 13*:2849–2861.

Kumar A, Ernst RR, Wüthrich K. 1980. A two-dimensional nuclear Overhauser enhancement (2D NOE) experiment for the elucidation of complete proton–proton cross-relaxation networks in biological macromolecules. *Biochem Biophys Res Commun 95*:1–6.

Lau SYM, Taneja AK, Hodges RS. 1984. Synthesis of a model protein of defined secondary and quaternary structure. Effect of chain length on the stabilisation and formation of two stranded α-helical coiled-coils. *J Biol Chem 259*:13253–13261.

Liu TY, Boykins RA. 1989. Hydrolysis of proteins and peptides in a hermetically sealed microcapillary tube: High recovery of labile amino acids. *Anal Biochem 182*:383–387.

Monera OD, Kay CM, Hodges RS. 1994. Electrostatic interactions control the parallel and antiparallel orientation of α-helical chains in two-stranded α-helical coiled-coils. *Biochemistry 33*:3862–3871.

O'Neil KT, DeGrado WF. 1990. A thermodynamic scale for the helix-forming tendencies of the commonly occurring amino acids. *Science 250*:646–651.

Richardson JS, Richardson DC. 1988. Amino acid preferences for specific locations at the ends of α helices. *Science 240*:1648–1652.

Robinson CR, Sligar SG. 1993. Electrostatic stabilization in four-helix bundle proteins. *Protein Sci 2*:826–837.

Rosen H. 1957. A modified ninhydrin colorimetric analysis for amino acids. *Arch Biochem Biophys 67*:10–15.

Royer CA, Chakerian AE, Matthews KS. 1990. Macromolecular binding equilibria in the *lac* repressor system: Studies using high-pressure fluorescence spectroscopy. *Biochemistry 29*:4959–4966.

Santoro MM, Bolen DW. 1988. Unfolding free energy changes determined by the linear extrapolation method. 2. Incorporation of $\Delta G^{\circ}_{N-V}$ values in a thermodynamic cycle. *Biochemistry 27*:8063–8067.

Sheridan RP, Levy RM, Salemme FR. 1982. α-Helix dipole model and electrostatic stabilization of 4-α-helical proteins. *Proc Natl Acad Sci USA 79*:4545–4549.

Shoemaker KR, Kim PS, York EJ, Stewart JM, Baldwin RL. 1987. Tests of the helix dipole model for stabilization of α-helices. *Nature 326*: 563–567.

Skolnick J, Holtzer A. 1982. Theory of helix–coil transitions of α-helical, two-chain coiled coils. *Macromolecules 15*:303–314.

Steif C, Weber P, Hinz HJ, Flossdorf J, Cesareni G, Kokkinidis M. 1993. Subunit interactions provide a significant contribution to the stability of the dimeric four-α-helical-bundle protein ROP. *Biochemistry 32*: 3867–3876.

Su YS, Hodges RS, Kay CM. 1994. Effect of chain length on the formation and stability of synthetic α-helical coiled coils. *Biochemistry 33*:15501–15510.

Terwilliger TC, Eisenberg D. 1982. The structure of melittin. I. Structure determination and partial refinement. *J Biol Chem 257*:6010–6015.

Thompson KS, Vinson CR, Freire E. 1993. Thermodynamic characterization of the structural stability of the coiled-coil region of the bZIP transcription factor GCN4. *Biochemistry 32*:5491–5496.

Wilcox W, Eisenberg D. 1992. Thermodynamics of melittin tetramerization determined by circular dichroism and implications for protein folding. *Protein Sci 1*:641–653.